

# Defining the instability strip of pulsating post-AGB binary stars from ASAS and NSVS photometry

L. L. Kiss<sup>1</sup>, A. Derekas<sup>1</sup>, Gy. M. Szabó<sup>2\*</sup>, T. R. Bedding<sup>1</sup>, L. Szabados<sup>3</sup>

<sup>1</sup>*School of Physics A28, University of Sydney, NSW 2006, Australia*

<sup>2</sup>*Department of Experimental Physics and Astronomical Observatory, University of Szeged, Hungary*

<sup>3</sup>*Konkoly Observatory of the Hungarian Academy of Sciences, Budapest, Hungary*

Accepted ... Received ... in original form ..

## ABSTRACT

We analyse public domain time-series photometric observations of 30 known and candidate binary post-AGB stars for measuring pulsation and orbital periods. We derive periodicities for 17 stars for the first time in the literature. Besides identifying five new RV Tauri type pulsating variables (three with the RVb phenomenon, i.e. long-term changes of the mean brightness), we find multiply periodic (or possibly irregular) post-AGB stars on the two edges of the instability strip. The temperature dependence of the peak-to-peak light curve amplitudes clearly indicates the changes in excitation as post-AGB stars evolve through the strip. One object, the peculiar Type II Cepheid ST Pup, showed a period increase from 18.5 to 19.2 d, which is consistent with the known period fluctuations in the past. In HD 44179, the central star of the Red Rectangle nebula, we see very similar asymmetric light curve than was measured 10–15 years ago, suggesting a very stable circumstellar environment. In contrast to this, HD 213985 shows coherent but highly non-repetitive brightness modulation, indicating changes in the circumstellar cloud on a similar time-scale to the orbital period.

**Key words:** stars: late-type – stars: supergiants – stars: oscillations – stars: evolution

## 1 INTRODUCTION

Post-AGB stars are rapidly evolving descendants of low and intermediate mass stars ( $\lesssim 8 M_{\odot}$ ). They are evolving at constant luminosity, crossing the Hertzsprung–Russell diagram from the cool Asymptotic Giant Branch (AGB) to the ionizing temperature of the planetary nebula nuclei, on a time-scale of about  $10^4$  years. During this process they cross the classical instability strip, in which large-amplitude radial oscillations are driven by the  $\kappa$ -mechanism, and the objects will be recognized as Type II Cepheids and RV Tauri type pulsating variables. Because of their fast evolution, these stars are rare and not many have been identified in the Galaxy (Van Winckel 2003).

The use of pulsations to determine the physical parameters of post-AGB stars has been very limited so far. Classical post-AGB variables, like (longer period) Type II Cepheids and RV Tauri stars, have an extensive literature and are understood to be low-order radial pulsators (for a review, see Wallerstein 2002). Some RV Tauri stars, the so-called RVb variables, also show long-term changes that are attributed to binarity. Although the MACHO database yielded important results on these objects (Alcock et al. 1998), the full use of microlensing data of post-AGB stars is yet to be explored.

The situation is much worse for post-AGB pulsators outside the Cepheid instability strip. Theoretical models have suggested that complex, possibly chaotic, pulsations should occur in stars hotter than the instability strip (Aikawa 1991, 1993; Gautschy 1993; Zalewski 1993). Indeed, irregular pulsations were found in several cases (Fokin et al. 2001; Le Coroller et al. 2003), but a comprehensive survey of many objects, using a homogeneous set of long-term observational data, has rarely been done so far (e.g. Pollard et al. 1996, 1997). This group of stars not only offer the possibility of measuring physical parameters via modelling oscillations, but they also offer the best opportunity to observe stellar evolution over human time-scales. Because these stars evolve quickly across the HRD, changes of their pulsation periods may be a sensitive indicator of the ongoing evolution, as in the extreme example of FG Sagittae (Jurcsik 1993).

De Ruyter et al. (2006) recently analysed broad-band Spectral Energy Distribution (SED) characteristics of a sample of post-AGB objects to investigate the presence of Keplerian rotating passive discs. The sample contained 51 stars, including confirmed binary post-AGB stars collected from the literature, classical RV Tauri stars from the General Catalog of Variable Stars (GCVS, Kholopov et al. 1985–1988) with strong infrared excess and a new sample of candidate RV Tauri stars (Lloyd Evans 1997). Based on the very similar SEDs they concluded that in all systems, gravitation-

\* Magyary Zoltán Postdoctoral Research Fellow

ally bound dusty discs are present, implying binarity of the central object. De Ruyter et al. (2006) used pulsations to estimate luminosities via the RV Tauri period–luminosity relation (Alcock et al. 1998). However, they only found pulsation periods in the literature for 21 stars, even though a much higher fraction of their sample resides in the instability strip. This lack of information prompted us to examine the publicly available photometric databases. Here we present our findings on photometric variability of the De Ruyter et al. sample.

## 2 THE SAMPLE AND DATA ANALYSIS

We used two all-sky photometric surveys as light curve sources: ASAS and NSVS. The third upgrade of All Sky Automated Survey (ASAS) has been covering 70% of the sky (everything south of  $+28^\circ$  declination) since 2000. As of writing, the ASAS-3 system has produced a few hundred individual  $V$ -band magnitude measurements for each of about 10 million stars, using two wide-field telescopes (200 mm telephoto lenses), located at the Las Campanas Observatory (see Pojmanski 2002 and references therein for details). The data have been online since the start of the observations and are available for download through the ASAS-webpage<sup>1</sup>. The useful magnitude range is between  $V = 8 - 14$  mag, although in some cases even brighter variables (e.g. U Mon) have good light curves, presumably due to shorter exposure times in these fields. The typical photometric errors (as indicated by the point-to-point scatter of long period variables) range from 0.01 to 0.2–0.4 mag, depending on the target brightness.

A limited northern counterpart to the ASAS was the Northern Sky Variability Survey (NSVS), which captured 1 year of the northern sky over the optical magnitude range from 8 to 15.5, providing typically 100–500 unfiltered measurements for approximately 14 million objects. The instrument was a wide-field telescope similar to that of the ASAS project and took data between 1999 April 1 and 2000 March 30 in Los Alamos, New Mexico (Wozniak et al. 2004). The NSVS public data release is available through a dedicated webpage<sup>2</sup>.

We searched the two online databases for the 30 stars that have no pulsation period given in Table A.2. of De Ruyter et al. (2006). We found useful data for 22 (mostly southern) of these in the ASAS-3 and for 2 northern/equatorial objects in the NSVS observations. In two cases (HR 4049 and HD 93662), the ASAS-3  $V$ -magnitudes showed large scatter that was probably caused by saturation. Nevertheless, one characteristic minimum was still identifiable for HR 4049 (see later). In addition, we also downloaded ASAS-3 data for 7 other pulsating stars that do have periods listed in Table A.2. of De Ruyter et al. (2006), so that we could check the consistency of our results with those in the literature.

The main properties of the final sample of 30 stars are summarized in Table 1. The mean time-span of the ASAS-3 light curves is 1682 days, although for 14 stars the time-base extends over 2000 days. With 300 datapoints in an average light curve, there is one ASAS-3 observation every few days, giving excellent coverage for stars with periods between 10 and 200 days. One of the two NSVS objects, QY Sge, was observed 120 times over the 1 year of operation, giving only a meagre picture of the variability, while NSVS data for IRAS 11472–0800 were useful in supplementing the information about the period change of the star.

**Table 1.** Stars in the sample and properties of the photometric datasets

IRAS	Other name	Sp. type	$\langle V \rangle$	JD from...to 2450000+	$N_{\text{obs}}$
05208–2035		M0e+F	9.46	1868...3869	336
06072+0953	CT Ori	F9I	10.47	2384...3865	168
06160–1701	UY CMa	G0V	11.03	1868...3881	332
06176–1036	HD 44179	F1I	8.84	1868...3880	285
06472–3713	ST Pup	F7I	10.01	1868...3896	346
07140–2321	SAO 173329	F5I	10.64	1868...3898	394
07284–0940	U Mon	G0I	6.46	1868...3896	299
08011–3627	AR Pup	F0I	9.38	1878...3897	327
08544–4431		F3	9.17	1868...3896	377
09060–2807	BZ Pyx	F5	10.86	1868...3898	328
09144–4933		G0	13.78	1868...3896	240
09256–6324	IW Car	F7I	8.50	1868...3897	1425
09400–4733		M0	10.56	1868...3896	327
09538–7622		G0	11.93	1870...3898	356
10158–2844	HR 4049	A6I	6.00	1871...3182	95
10174–5704		K:rr	11.30	1868...3190	270
10456–5712	HD 93662	K5	6.60	1868...3223	421
11000–6153	HD 95767	F0I	8.79	1869...3231	218
11472–0800		F5I	11.58	1871...3189	167
				1274...1634	114*
12222–4652	HD 108015	F3Ib	7.95	1954...3239	137
15469–5311		F3	10.55	1936...3262	257
17038–4815		G2p(R)e	10.53	1933...3288	251
17233–4330		G0p(R)	12.26	1936...3260	178
17243–4348	LR Sco	G2	10.50	1933...3260	215
17530–3348	AI Sco	G4I	9.83	2417...3293	118
18123+0511		G5	10.14	2159...3292	121
19125+0343		F2	10.16	2138...3896	209
19157–0247		F3	10.72	1979...3896	235
20056+1834	QY Sge	G0 De	10.8*	1277...1632	120*
22327–1731	HD 213985	A2I	8.92	1871...3897	284

\* – unfiltered magnitudes from the NSVS project

We determined periods by iterative sine-wave fitting using PERIOD04 of Lenz & Breger (2005). In several stars the variations are too complex for simple stationary Fourier-fits. In those cases we fitted harmonic components with variable frequencies using our own codes. Examples of power spectra are plotted in Fig. 1. The uncertainties of the determined periods were conservatively estimated from the spectral window by taking its full width at half maximum as the error in frequency. For the RV Tauri type stars, after finding the mean period, we fitted a fixed set of integer multiplets of the mean frequency to describe the highly non-sinusoidal light curve shapes. That was an approximation for most RV Tau stars, because their light curve cycles are well-known for not being strictly repetitive. In Figs. 2–4 we show 27 of the resulting light curve fits.

## 3 RESULTS

All of the objects in the sample turned out to be photometrically variable (note that the ASAS-3 catalog contains all the observed stars, not only the variable ones). It is apparent from Figs. 2–4 that the sample has a very rich photometric behaviour. In most cases we could determine at least one period, while in 13 stars we infer multiple periodicity with a wide range of period ratios. In cooler (and hence larger amplitude) stars, the long secondary periods correspond to the so-called RVb phenomenon, i.e. long-term changes of the mean brightness, coupled with the short-term RV Tauri pulsations. We identify five new genuine RV Tauri variables, whose RV Tauri nature was suggested by their position in the IRAS two-colour diagrams (Lloyd-Evans 1997). In a few objects we see several cases of beating, caused by multiple frequencies with ratios between 1.0 and 2.0. In those cases we determined 2 or 3 periods, although we note that the time-span of the data is not long enough

<sup>1</sup> <http://archive.princeton.edu/~asas>

<sup>2</sup> <http://skydot.lanl.gov/nsvs/nsvs.php>

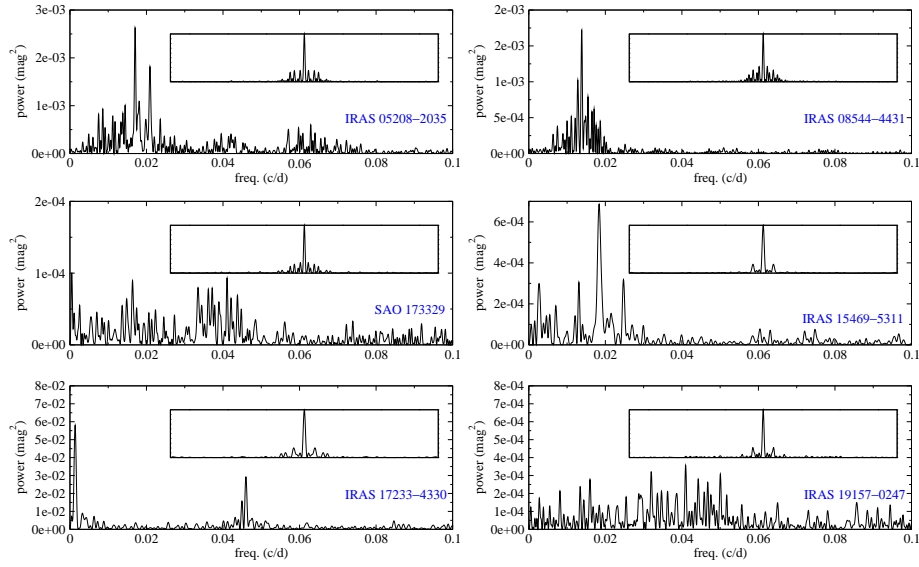
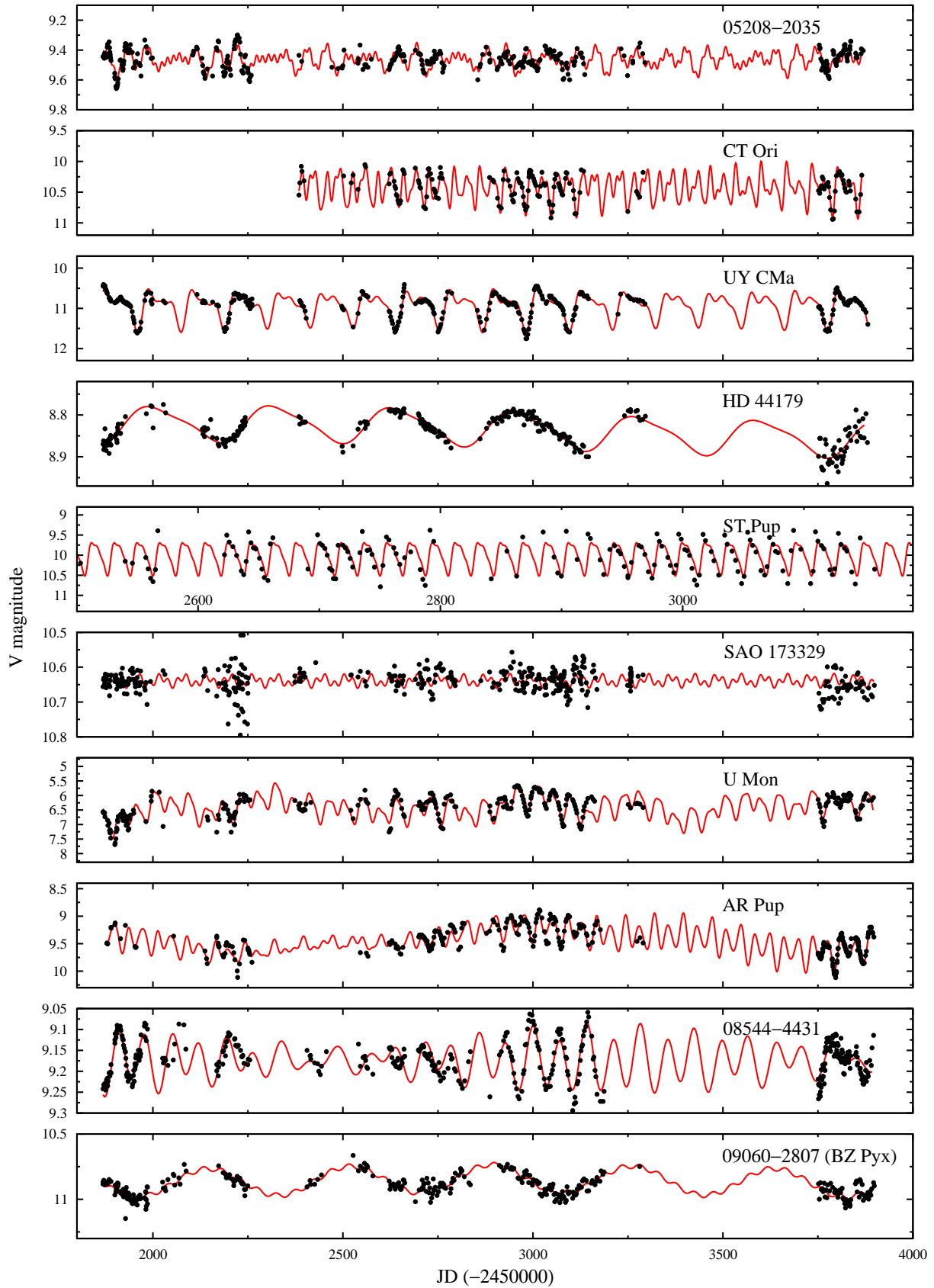


Figure 1. Sample power spectra. The insets show the spectral window on the same scale.

**Table 2.** Stellar parameters (taken from De Ruyter et al. 2006),  $V$ -band amplitude (to the nearest 0.05-0.1 mag) and the determined periods with  $S/N > 4$ . Key to the variability types: ‘RVa’ – RV Tauri pulsator with constant mean brightness; ‘RVb’ – RV Tauri pulsator with varying mean brightness; Cep II – Population II Cepheid; ‘pulsating’ – low amplitude semiregular or multiply periodic variable; ‘binary’ – photometric variations with the orbital period; Irr – variable without well-defined pattern (irregular).

IRAS	Other name	$T_{\text{eff}}$	$\log g$	[Fe/H]	$\Delta V$ [mag]	Period(s) (this study) [d]	Type of variability	Period(s) (literature) [d]	ref.
05208–2035		4000	0.5	0.0	0.2	58.8±0.9, 47.6±0.6 117±2.5, 15.6±0.7	pulsating	—	–
06072–0953	CT Ori	5500	1.0	–2.0	0.8	67.3±1	RVa	135.52	1
06160–1701	UY CMa	5500	1.0	0.0	1.1	113.7±2.5	RVa/Cep II	113.9	1
06176–1036	HD 44179	7500	0.8	–3.3	0.1	319±20 + 2nd harmonic	binary	318±3	2
06472–3713	ST Pup	5750	0.5	–1.5	1.1	changing from 18.5 to 19.2 d	Cep II	18.88	1
07140–2321	SAO 173329	7000	1.5	–0.8	0.05	~60, ~24	Irr	—	–
07284–0940	U Mon	5000	0.0	–0.8	1.1	91.3±2.3	RVb	92.26	1
08011–3627	AR Pup	6000	1.5	–1.0	0.5	76.4±4, 1250±300	RVb	75	1
08544–4431		7250	1.5	–0.5	0.12	72.3±1.3, 68.9±1.2, 133±1	pulsating	499±3, 72 or 90	3
09060–2807	BZ Pyx	6500	1.5	–0.5	0.2	372±35, 48±6	RVb	—	–
09144–4933		5750	0.5	–0.5	0.6	93±2	pulsating	—	–
09256–6324	IW Car	6700	2.0	–1.0	0.4	72.1±1, 1400±500, 42±0.5	RVb	67.5	1
09400–4733					0.1	~1300, ~200	pulsating	—	–
09538–7622		5500	1.0	–0.5	1.0	1190±300, 100.6±2.5	RVb	—	–
10158–2844	HR 4049	7500	1.0	–4.5	>0.5	one characteristic minimum	binary	434	4
10174–5704					1.0	time-scale of 500–600 d	binary?	—	–
10456–5712	HD 93662	4250	0.5	0.0	>0.5	two maxima ~260 d apart, scatter	binary?	—	–
11000–6153	HD 95767	7600	2.0	0.1	0.1	92±2 (~2000)	pulsating	—	–
11472–0800		5750	1.0	–2.5	0.6	31.5±0.6	Cep II	—	–
12222–4652	HD 108015	7000	1.5	–0.1	0.1	61±1.9, 55±1.6	pulsating	—	–
15469–5311		7500	1.5	0.0	0.1	54.4±1, 384±50, 49.1±0.8	pulsating	—	–
17038–4815		4750	0.5	–1.5	1.5	75.9±1.9	RVa	—	–
17233–4330		6250	1.5	–1.0	0.5	735±230, 44±0.8	RVb	—	–
17243–4348	LR Sco	6250	0.5	0.0	0.8	100.5±4	RVa	104.4	5
17530–3348	AI Sco	5000	0.0	0.0	1.0	71.6±5.1, ≈ 870	RVb	71.0	1
18123+0511		5000	0.5	0.0	0.6	172±15	RVa	—	–
19125+0343		7750	1.0	–0.5	0.05	~2300, time-scale of 50 d	pulsating	—	–
19157–0247		7750	1.0	0.0	0.05	~25 d	Irr	—	–
20056+1834	QY Sge	5850	0.7	–0.4	–	four minima at ~60 d separation	pulsating	~50	6
22327–1731	HD 213985	8250	1.5	–1.0	0.4	261.5±17 + 2nd harmonic	binary	254	7



**Figure 2.** ASAS V-band light curves of post-AGB stars. Solid lines denote low-order harmonic fits. For clarity we expanded the time-axis for ST Pup, thus showing only half of the ASAS data.

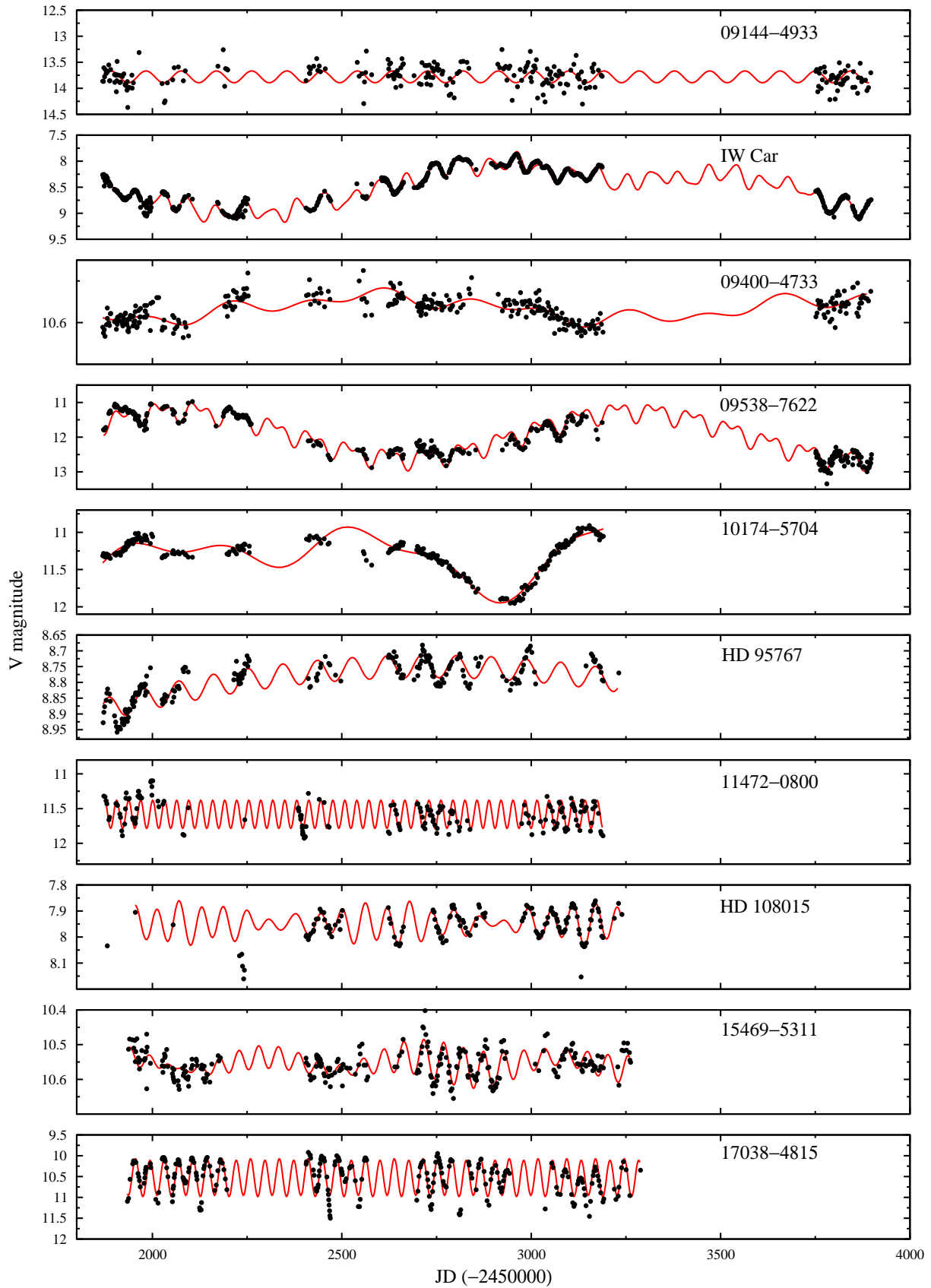
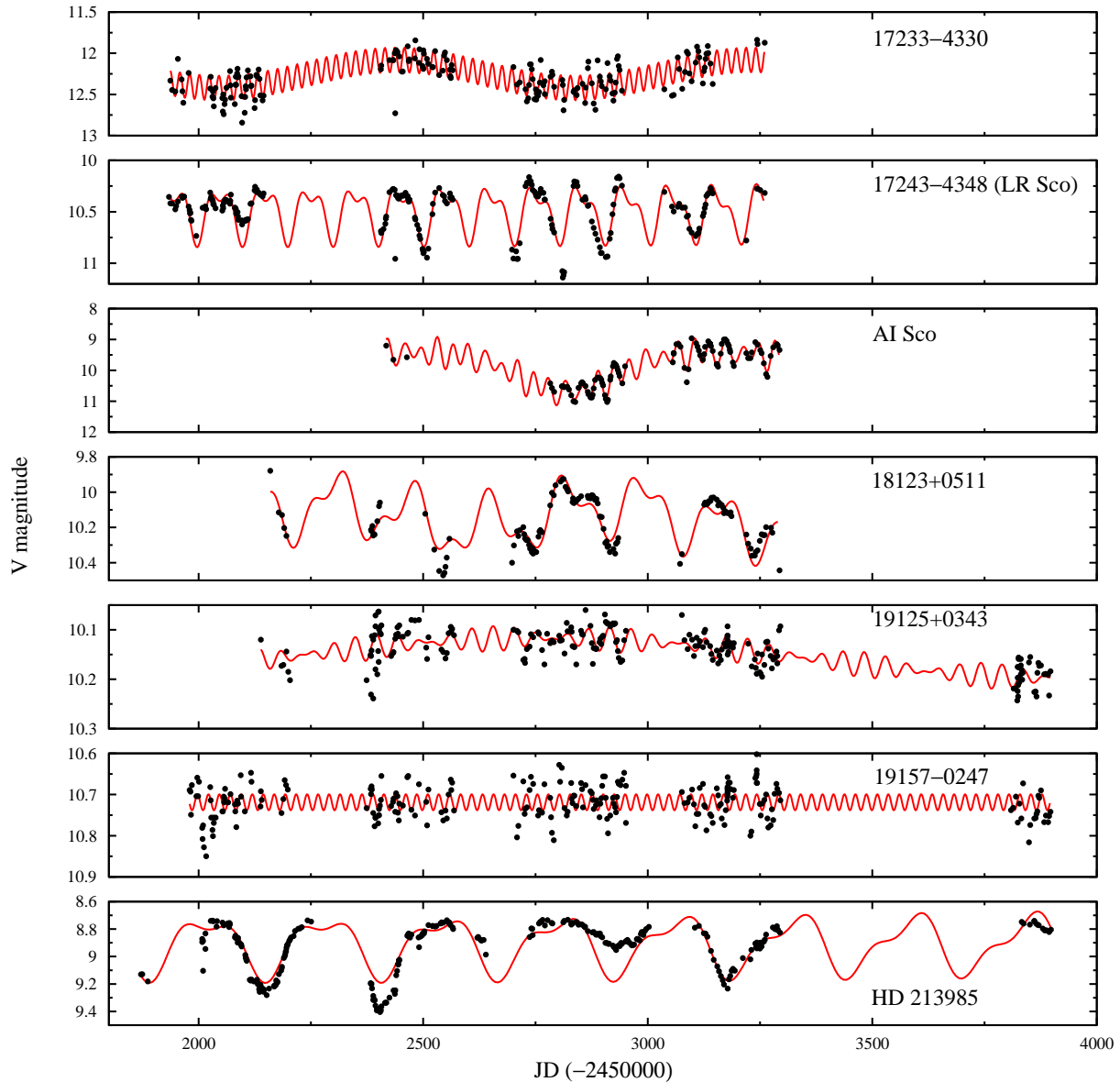


Figure 3. ASAS V-band light curves and harmonic fits of post-AGB stars.



**Figure 4.** ASAS  $V$ -band light curves and harmonic fits of post-AGB stars.

to make a distinction between non-repetitive quasi-regularity and genuine multiple periodicity.

We present stellar parameters and periods in Table 2. Detailed notes on each star are given in Appendix A.

#### 4 DISCUSSION

Our study aimed at determining periods for a well-defined sample of post-AGB stars, which includes confirmed and candidate binary objects. The homogeneous set of ASAS-3  $V$ -band data allowed us to study photometric variability with an extended coverage of this interesting evolutionary phase. The immediate result is an improved knowledge about pulsations and orbital brightness modulations in a relatively large set of post-AGB stars. Let us recall that the most extensive catalogue contains about 220 objects (Szczerba et al. 2001), so that our 30 stars form a significant fraction of post-AGB stars known to date. By restricting our investigation to the De

Ruyter et al. (2006) sample, we ensured that the properties of all stars are known to similar accuracy.

Almost half of the sample comprises RV Tau-type pulsating variables, of which five are new identifications. Assuming that the RVb phenomenon is a signature of orbital modulations, we have measured the orbital periods for three stars (BZ Pyx: 372 d; IRAS 09538–7622: 1190 d; IRAS 17233–4330: 735 d). Their confirmation will require long-term spectroscopic monitoring. In three more RVb stars (AR Pup, IW Car and AI Sco) we measured modulation periods that are consistent with those in the literature.

We find two new candidates for binary modulations (IRAS 10174–5704 and HD 93662) to add to the well-known examples of HD 44179, HR 4049 and HD 213985. Unfortunately, in neither case are the data long or accurate enough to derive orbital periods. We can only say that the time-scales are a few hundred days. Of the known binary variables, HD 213985 is most interesting for future monitoring because of the cycle-to-cycle changes of

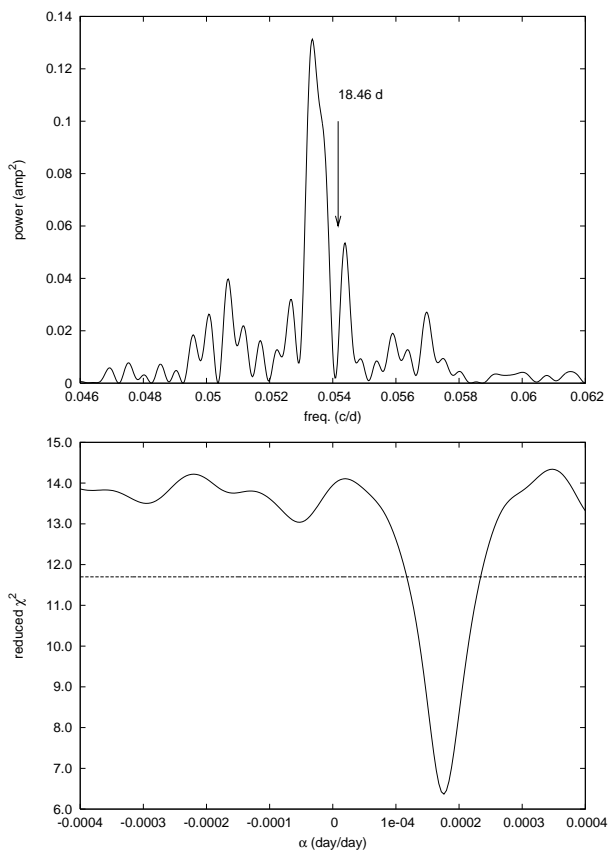


**Figure 5.** *Top panel:* a close-up view of the power spectrum of ST Pup. The arrow marks the mean period around the early 1990s (Gonzalez & Wallerstein 1996). Side-lobe peaks come from the spectral window. *Bottom panel:* reduced  $\chi^2$  as a function of the linear period evolution parameter  $\alpha$ , assuming  $P(t) \sim P_0 + \alpha t$ . The dashed line shows the  $\chi^2$  of the best monoperoiodic fit.

the light curve shape. This behaviour suggests on-going changes in the circumstellar shell, and high-resolution observations may shed new light on the mass-loss processes in post-AGB binaries.

#### 4.1 Stars with period variations

One star in the sample, the peculiar Pop. II Cepheid ST Pup, has long been known to show long-term fluctuations in period that are not consistent with evolutionary theories (Wallerstein 2002) and for which there is no firm theoretical explanation. ST Pup might be similar to V725 Sgr, which first increased its period from 12 d to 21 d between 1926 and 1935 and then, most recently, up to 90 d, representing a blue loop in the HRD from the AGB to the instability strip and back again (Percy et al. 2006).

The ASAS photometry indicates a strongly changing pulsation period with a linear increase of  $\alpha = dP/dt = 1.75 \times 10^{-4}$  day/day (see Fig. 5). Note that this result is based on the simple assumption of linear period change, which is not valid for the whole history of ST Pup. Gonzalez & Wallerstein (1996) determined the orbital period of this system from radial velocity data to be 410.4 days. The value of orbital periodicity, however, strongly depends on the radial velocity variations caused by the pulsation. When decomposing the radial velocity changes into pulsational and orbital components, it is essential to use the correct pulsation period de-

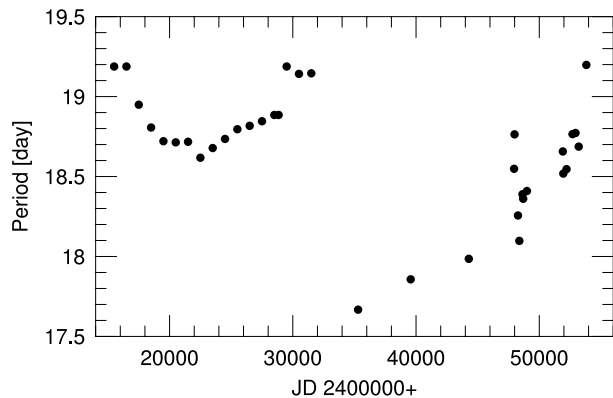


**Figure 6.** The pulsation period of ST Puppis varies erratically. This Type II Cepheid shows both smooth and violent period changes incompatible with evolutionary effects.

rived from photometry. From the present period study it is obvious that the pulsation period of 18.4622 days used by Gonzalez & Wallerstein was incorrect for the epoch of their radial velocity observations. Instead, the value of 18.4298 day is a reasonable approximation. Decomposing the radial velocity data with this latter period, a much shorter period emerges for the orbital periodicity, instead of 410.4 days, the value of 25.67 days fits much better the radial velocity data prewhitened with the variations of pulsational origin. Such a short orbital period (if confirmed) means that the secondary star can influence the pulsation significantly and offers a natural explanation for the instability of the pulsation period of ST Puppis.

These strong period changes in ST Puppis occurring on a short time scale prompted us to study the behaviour of the pulsation period of this particular Cepheid using all available photometric data. The period for the first half of the 20th century was published by Payne Gaposchkin (1950). In general, the period was longer than now and the changes in it were apparently less sudden as compared with the recent behaviour. Reliability of these period values is supported by an independent period determination made by Hoffmeister (1943) based on another series of photographic observations. From the mid-20th century on, data have been obtained with photoelectric equipment and, more recently with CCD cameras. Because the individual data are all accessible, a homogeneous treatment is possible for determining the instantaneous pulsation period. The data series analysed included (in the order of the epoch of observations) the observations by Irwin (1961), Wallraven, Muller & Oosterhoff (1958), Landolt (1971), Harris (1980), Kilkeny et al. (1993), the Hipparcos satellite (ESA 1997), and Berdnikov & Turner (2001). At first, the periods were determined separately for each dataset (photometric samples covering several years were divided into reasonably short segments). The temporal dependence of the pulsation period is plotted in Figure 6. The uncertainties of the individual period values are smaller than the size of the circles. It is seen that violent period changes are superimposed on the smooth (yet strong) variations of the pulsation period. Most conspicuous jumps in the period occurred between JD 2 432 000 and JD 2 435 000, near JD 2 449 000, and between JD 2 453 000 and JD 2 454 000. This erratic behaviour is incompatible with stellar evolution across the instability strip. Whether it has to do with the presence of a companion is a question that must be answered by dedicated observations.

Another Pop. II Cepheid, IRAS 11472–0800 exhibited quite

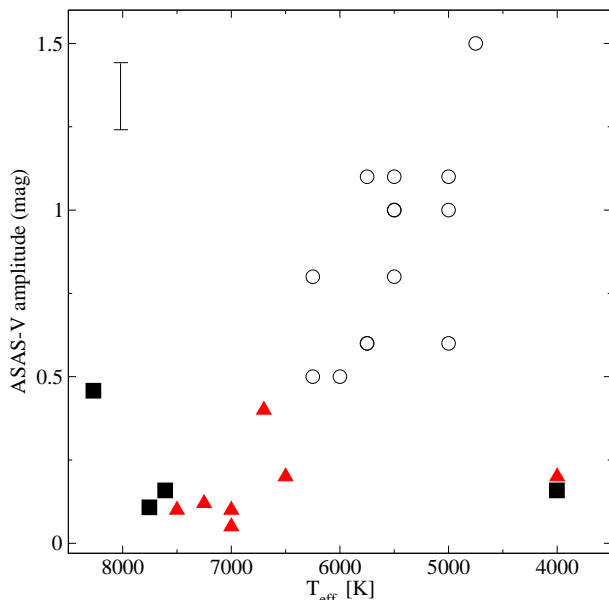


**Figure 7.** *V*-band amplitude as a function of effective temperature for post-AGB variables. Open circles: single periodic stars; triangles: multi-periodic/semiregular stars; squares: variability due to orbital motion. The bar in the upper left corner shows the typical cycle-to-cycle amplitude variation in the pulsating stars.

strong phase modulations without a clear long-term trend (see the Appendix for details). We find no star in the sample with FG Sge-like period change that might be due to the final helium flash during post-AGB evolution (e.g. Blöcker & Schönberner 1997). A comprehensive analysis of all post-AGB stars identified to date in the available photometric surveys, most importantly in the ASAS database, will be an important future task.

#### 4.2 The pulsations of post-AGB stars

In Fig. 7 we show peak-to-peak amplitudes of the ASAS-3 light curves versus effective temperature (cf. fig. 1 of Lloyd Evans 1999). For the RVb stars, we first removed the long-term modulation. Since the effective temperature is a good indicator of the post-AGB evolutionary phase, the correlation between the *V*-band amplitudes and  $T_{\text{eff}}$  is a spectacular indication of how post-AGB stars evolve through the instability strip. The temperatures were taken from De Ruyter et al. (2006), who determined a consistent set of stellar photospheric temperatures for the majority of the sample from high-resolution spectra. For RV Tauri stars they deduced the parameters from spectra taken preferentially around the maximum light, when the effects of the molecular bands are weaker. In Fig. 7 we made a distinction between singly periodic and multiply periodic (or possibly semiregular) variables to show how pulsation behaviour changes on the two edges of the instability strip. Note that for the coolest RV Tau stars the *V*-band amplitude is enhanced by the temperature sensitivity of the molecular bands in the optical spectrum. However, for temperatures above 5000 K, where most of the stars lie, we expect the effect to be small.

We draw several conclusions based on Fig. 7. The position of the instability strip is very well-defined by the boundaries at  $\approx 4500$  K and 6500 K. This is where the higher amplitude Type II Cepheid/RV Tauri pulsations are excited by the  $\kappa$ -mechanism. For stars that have left the instability strip, the pulsations are much

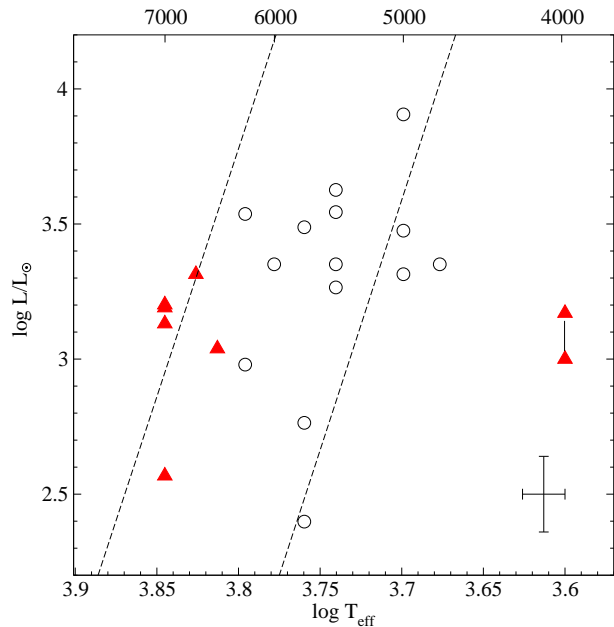


**Figure 8.** The empirical HRD of the pulsating sample, using the RV Tau period–luminosity relation in the Large Magellanic Cloud. The dashed lines show the edges of the classical instability strip, taken from Christensen-Dalsgaard (2003). The error bars in the lower right corner represent  $\pm 3\%$  error in effective temperature (about 200 K in the range shown) and the  $\pm 0.35$  mag standard deviation of the LMC P–L relation.

less dynamic and regular. However, the lack of a sharp edge on the hot side is exactly as predicted by model calculations (Aikawa 1993, Gautschy 1993). It is very interesting that a similar behaviour may occur for the red edge, too, although the evidence is based on a single object (IRAS 05208–2035). Despite the lack of stars between 4000 K and 4750 K, the asymmetric amplitude distribution suggests a narrower red edge for the instability strip, which might be understood in terms of a stronger damping by convection in the cooler stars.

To place our stars in the Hertzsprung–Russell diagram, we have used the period–luminosity relation for RV Tauri stars in the Large Magellanic Cloud derived by Alcock et al. (1998), which has been used by De Ruyter et al. (2006) for estimating the luminosities of the pulsating objects in their sample. We used the same P–L relation to calculate *V*-band absolute magnitudes:

$$M_V = 2.54(\pm 0.48) - (3.91 \pm 0.36) \log(P/2), \quad \sigma = 0.35$$

for variables with  $P/2 > 12.6$  days. To calculate luminosities, we took  $BC_V$  values from Table A.2 in De Ruyter et al. (2006). The resulting empirical HRD is shown in Fig. 8, where we also show the boundaries of the classical instability strip, adopted from Christensen-Dalsgaard (2003). We did not include stars hotter than 7000 K because the applicability of the RV Tau P–L relation becomes doubtful for stars that have parameters outside the calibrating sample. This is also true for the coolest multiply periodic star on the right-hand side in Fig. 8 (IRAS 05208–2035), but its position in the plot could still be interesting, so we applied the P–L relation to both of the periods.

Fig. 8 reveals a very nice agreement with the classical instability strip. Using other models of the Cepheid instability strip (e.g. Saio & Gautschy 1998; Baraffe et al. 1998; Bono et al. 2005) gives slight changes in the slope and exact locations of the theoretical edges but does not change the overall agreement. This means that



the LMC RV Tau P–L relation and the adopted spectroscopic temperature estimates, both free of any theoretical assumption on the pulsations, yield a consistent physical picture of post-AGB stars evolving through the instability strip (see also Lloyd Evans 1999). Interestingly, there is a suggestion for a more extended red edge from the outside positions of the three coolest and largest amplitude RV Tau stars (near the location  $\log T_{\text{eff}} = 3.7$ ,  $\log L/L_{\odot} = 3.4$ ). This becomes more evident if we consider that the temperatures of those stars were determined in the hottest states, so that their mean temperatures are even cooler. We interpret this subtle difference as one caused by the different stellar structure of Cepheids and post-AGB stars. They may overlap in temperature and luminosity, but Cepheids are massive stars (5–8  $M_{\odot}$ ), which means their density profile will be different from that of the post-AGB objects. Therefore, we do not expect the same efficiency of excitation at a given position of the HRD, especially at the edges of the instability strip.

Finally, some of the objects on the blue edge of the instability strip present evidence for multiply periodic oscillations with period ratios around 1.1 (cf. Fig. 1). The simplest explanations are the presence of radial and non-radial modes or of very high-order radial modes. The former case could be interesting in the search for mechanisms that may lead to non-spherical mass-loss (e.g. Soker 2000). These are also the objects for which asteroseismology could be very rewarding, provided that realistic models are calculated for a wide range of parameters (see Fokin et al. 2001).

## ACKNOWLEDGMENTS

This work has been supported by a University of Sydney Post-doctoral Research Fellowship, the Australian Research Council, the Hungarian OTKA Grants #T042509, #T046207 and the Magyar Zoltán Public Foundation for Higher Education. The ASAS and NSVS online catalogues and the NASA ADS Abstract Service were used to access data and references. This research has made use of the SIMBAD database, operated at CDS-Strasbourg, France.

## REFERENCES

- Aikawa, T., 1991, *ApJ*, 374, 700  
Aikawa, T., 1993, *MNRAS*, 262, 893  
Alcock, C., et al., 1998, *AJ*, 115, 1921  
Baraffe, I., Alibert, Y., Méra, D., Chabrier, G., Beaulieu, J.-P., 1998, *ApJ*, 499, L205  
Berdnikov, L.N., & Turner, D.G., 2001, *ApJS*, 137, 209  
Blöcker, T., & Schönberner, D., 1997, *A&A*, 324, 991  
Bono, G., Marconi, M., Cassisi, S., Caputo, F., Gieren, W., & Pietrzynski, G., 2005, *ApJ*, 621, 966  
Christensen-Dalsgaard, J., 2003, *Lecture Notes on Stellar Oscillations*, Aarhus University, May 2003, Fifth edition (<http://astro.phys.au.dk/~jcd/oscilnotes>)  
De Ruyter, S., Van Winckel, H., Maas, T., Lloyd Evans, T., Waters, L.B.F.M., & Dejonghe, H., 2006, *A&A*, 448, 641  
Eggen, O.J., 1986, *AJ*, 91, 890  
ESA, 1997, *The Hipparcos Catalogue*, ESA SP-1200  
Fokin, A.B., Lèbre, A., Le Coroller, H., & Gillet, D., 2001, *A&A*, 378, 546  
Gautschi, A., 1993, *MNRAS*, 265, 340  
Giridhar, S., Rao, N.K., & Lambert, D.L., 1992, *JApA*, 13, 307  
Giridhar, S., Rao, N.K., & Lambert, D.L., 1994, *ApJ*, 437, 476  
Giridhar, S., Lambert, D.L., Bacham E., R., Gonzalez, G., Yong, D., 2005, *ApJ*, 627, 432  
Gonzalez, G., & Wallerstein, G., 1996, *MNRAS*, 280, 515  
Harris, H.C., 1980, PhD Thesis, Univ. of Washington  
Hashimoto, O., 1994, *A&AS*, 107, 445  
Hoffmeister, C., 1930, *AN*, 238, 17  
Hoffmeister, C., 1943, *Kl. Veröff. Berlin-Babelsberg*, No. 27, 47  
Horowitz, D.H., 1986, *JAAVSO*, 15, 223  
Irwin, J.B., 1961, *ApJS* 6, 253  
Jurcsik, J., 1993, *Acta Astron.*, 43, 353  
Kazarovets, E.V., Samus, N.N., & Durlевич, O.V., 2001, *IBVS*, 5135  
Kholopov, P.N., et al., 1985-1988, *General Catalogue of Variable Stars (GCVS)*, 4th edition, Nauka, Moscow  
Kilkenny D., et al., 1993, *SAAO Circ.*, No. 15, 85  
Lake, R., 1963, *MNSSA*, 22, 79  
Landolt, A.U., 1971, *PASP*, 83, 43  
Le Coroller, H., Lèbre, A., Gillet, D., & Chapellier, E., 2003, *A&A*, 400, 613  
Lenz, P., & Breger, M., 2005, *Comm. Asteroseis.*, 146, 53  
Lloyd Evans, T., 1997, *Ap&SS*, 251, 239  
Lloyd Evans, T., 1999, *IAU Symp.* 191, 453  
Maas, T., et al., 2003, *A&A*, 405, 271  
Menzies, J.W., & Whitelock, P.A., 1988, *MNRAS*, 233, 697  
Payne Gaposchkin, C., 1950, *HA*, 115, 205  
Percy, J.R., Molak, A., Lund, H., Overbeek, D., Wehlau, A.F., Williams, P.F., 2006, *PASP*, 118, 805  
Pojmanski, G., 2002, *Acta Astron.*, 52, 397  
Pollard, K.R., & Cottrell, P.L., 1995, *ASP Conf. Series*, 83, 409  
Pollard, K.R., Cottrell, P.L., Kilmartin, P.M., & Gilmore, A.C., 1996, *MNRAS*, 279, 949  
Pollard, K.R., Cottrell, P.L., Lawson, W.A., Albrow, M.D., & Tobin, W., 1997, *MNRAS*, 286, 1  
Rao, N.K., Goswami, A., & Lambert, D.L., 2002, *MNRAS*, 334, 129  
Raveendran, A.V., 1999, *MNRAS*, 303, 595  
Saio, H., & Gautschi, A., 1998, *ApJ*, 498, 360  
Soker, N., 2000, *MNRAS*, 312, 217  
Szczerba, R., Górny, S.K., & Zalfresso-Jundziłło, M., 2001, *Astrophys. Space Sci. Library*, Vol. 265, 13  
Van Winckel, H., 2003, *ARA&A*, 41, 391  
Van Winckel, H., Waelkens, C., & Waters, L.B.F.M., 2000, *IAU Symp.*, 177, 285  
Waelkens, C., et al., 1991, *A&A*, 242, 433  
Waelkens, C., Van Winckel, H., Waters, L.B.F.M., & Bakker, E.J., 1996, *A&A*, 314, L17  
Wallerstein, G., 2002, *PASP*, 114, 689  
Walraven, Th. Muller, A.B., & Oosterhoff, P.Th., 1958, *BAN*, 14, 81  
Whitelock, P.A., et al., 1989, *MNRAS*, 241, 393  
Woźniak, P.R., et al., 2004, *AJ*, 127, 2436  
Zalwski, J., 1993, *Acta Astron.*, 43, 431

## APPENDIX A: NOTES ON INDIVIDUAL STARS

Except where noted, nothing has previously been published on the variability of most of these stars.

**IRAS 05208–2035:** This star belongs to the candidate RV Tauri stars based on the position in the IRAS colour-colour diagram of Lloyd Evans (1997). Previously, Hashimoto (1994) listed the star among oxygen-rich AGB stars. The light curve (Fig. 2) is dominated by short-period, complex variations with time-scales from 16 d to 120 d, which are hardly compatible with typical AGB stars. None of these periods comes from a coherent signal that might have indicated orbital motion.

**CT Ori:** De Ruyter et al. (2006) listed a period of 135 d, which can be traced back to Hoffmeister (1930), but which is not correct. It was already pointed out by Horowitz (1986) that the period is more likely to be half or even a quarter of that. The ASAS data (Fig. 2) clearly shows alternating light curve with 67 days between two consecutive primary minima.

**UY CMa:** We confirm the catalogued period of  $\sim 114$  d.

**HD 44179:** This binary is the central star of the Red Rectangle nebula, with an orbital period of  $318 \pm 3$  d. Waelkens et al. (1996) measured an asymmetric light curve with 0.12 mag amplitude in  $V$  and no colour variation over the optical range. Their data, taken over six orbital cycles, revealed only minor light curve shape changes, suggesting a stable configuration of the inner circumstellar disk. Waelkens et al. (1996) proposed that photometric variability is not caused by variable extinction due to the orbital motion (as was commonly assumed) but by the variation around the orbit of the scattering angle of the light that is observed. Our analysis confirms the period and, apart from a tiny zero-point shift of the photometry, we find a very similar light curve to that measured by Waelkens et al. (1996) more than a decade earlier (Fig. 2). This suggests stable conditions around the binary over the whole baseline of about two decades. The power spectrum does not contain any excess power that could be indicative of low-amplitude pulsations.

**SAO 173329:** We find that this star is variable at the 0.1 mag level. The light curve (Fig. 2) is rather irregular; the listed “periods” are time-scales of dimmings rather than real periods.

**U Mon:** This is a well-known RV Tau variable of the ‘b’ subtype. The ASAS data (Fig. 2) are not long enough to detect the  $\sim 2600$  d modulation of the mean brightness, which was identified as the orbital period of the system (Pollard & Cottrell 1995).

**AR Pup:** We confirm both the known 75 d pulsation period and the RVb modulation period of  $\sim 1200$  d (Raveendran 1999; see Fig. 2).

**IRAS 08544–4431:** Maas et al. (2003) measured an orbital period of  $499 \pm 3$  d and found two periods of nearly equal probability, 71.9 d and 89.9 d. The ASAS light curve (Fig. 2) confirms the shorter pulsation period (72 d) as well as a slightly shorter one (69 d), producing a clear beat. The presence of a third significant period ( $S/N > 4$  for 133 d) that is close to the twice the shortest one, supports the multi-mode interpretation of the apparent amplitude modulation. Despite covering 4 orbital cycles, the light curve does not show evidence for orbital brightness variations.

**BZ Pyx:** The variable star designation and class SR: were given by Kazarovets, Samus & Durlevich (2001), who referred to a VSNET report by K. Takamizawa in 2000, in which the discovery of new field variable stars was announced with no period determination. The ASAS light curve (Fig. 2) suggests two periods and resembles an RVb type pulsation with long-term modulation, except that the pulsation amplitude and period are far smaller than in typical RVb stars. The regularity of the modulation suggests that the  $372 \pm 1$  d period corresponds to orbital motion.

**IRAS 09144–4933:** The SIMBAD database lists this as an RV Tau variable, but no reference or period are given. The star is quite faint for the ASAS instrument, which is the reason for the high point-to-point noise in the light curve (Fig. 3). Although the determined period would be typical for an RV Tau star, the light curve is too noisy for a firm classification.

**IW Car:** This star is a C-rich RVb variable with a 67.5–80 d pulsation and 1500 d modulation period (Giridhar, Rao & Lambert 1994). The latter is confirmed by the ASAS data, while the short-period oscillations are best described with periods of 72 d and 42 d

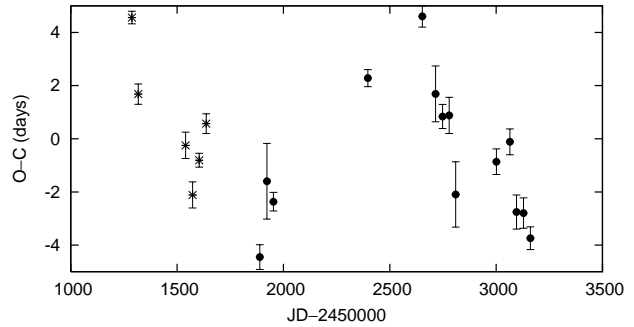


**Figure A1.** Cycle-to-cycle phase variations of IRAS 11472–0800 from NSVS (stars) and ASAS-3 (dots) data.

(Fig. 3). However, the shorter one, being close to the harmonic of the main period, might only be caused by the non-sinusoidal shape of a non-stationary signal.

**IRAS 09400–4733:** The light curve (Fig. 3) shows slow fluctuations but the overall behaviour does not seem to be periodic.

**IRAS 09538–7622:** We find this star to be a typical RVb type pulsating star with well-defined modulation period close to 1200 d (Fig. 3).

**HR 4049:** Waelkens et al. (1991) found a periodicity of 434 d, which was interpreted as an orbital period. The star is bright ( $V < 6$  mag) and the ASAS data seem to have been affected by saturation. Nevertheless, one characteristic minimum was observed around JD 2452800, which extended over 200 d and had a very similar shape to those observed by Waelkens et al. (1991).

**IRAS 10174–5704:** The ASAS light curve (Fig. 3) shows variations up to 1 mag with a characteristic time-scale of 500–600 d.

**HD 93662:** Lake (1963) suspected its variability (hence the designation NSV 4975) but nothing specific has been published since then. The ASAS data have large scatter, presumably from saturation effects, but two minima about 260 d apart are still recognizable.

**HD 95767:** The light curve (Fig. 3) clearly shows a small-amplitude oscillation with 92 d period and a gradual change of the mean brightness that could indicate a modulation period of  $\sim 2000$  d.

**IRAS 11472–0800:** This is a relatively low-amplitude Type II Cepheid with 31.5 d pulsation period (Fig. 3). We find quite strong phase variations up to  $\pm 5$  d or 0.16 pulsation phase (Fig. A1).

**HD 108015:** This is a bright, low-amplitude, multiply periodic pulsator (Fig. 3) with no previous variability study.

**IRAS 15469–5311:** Very similar to HD 108015 in its variability (Fig. 3).

**IRAS 17038–4815:** This star has been included in the abundance analysis of an extended sample of field RV Tau stars (Giridhar et al. 2005), with no specific variability information given. The light curve shows typical RV Tau variations with 76 d period (Fig. 3).

**IRAS 17233–4330:** We derive variability parameters for the first time. Besides a long-term modulation (Fig. 4), the light curve shows 0.5 mag oscillations with a formal period of 22 d. However, tiny differences in minima suggest a doubled period of 44 d, which puts the star among the RVb type variables.

**LR Sco:** First misclassified as R CrB star then realized it was a yellow semiregular variable (Giridhar, Rao & Lambert 1992). We determine a period that is close to the one in the GCVS. The light curve shape is typical of an RV Tau star (Fig. 4).

**AI Sco:** We measure a very similar pulsation period than listed by De Ruyter et al. (2006), which originates from Pollard et al. (1996). These authors measured a long (RVb) period of 940 d, which is not entirely inconsistent with the ASAS data, especially if we consider their short time-span ( $<900$  d, see Fig. 4).

**IRAS 18123+0511:** We find this to be an RV Tau-like variable (Fig. 4). Its period is somewhat long and the amplitude is low for a typical RVa-type star.

**IRAS 19125+0343:** The SIMBAD database lists as a variable star of RV Tau type, but neither the period, nor the source of information is given. Besides a short period and low amplitude fluctuation we also find a long-term modulation (Fig. 4).

**IRAS 19157–0247:** We find tiny fluctuations just above the noise (Fig. 4) but the determined time-scale is not a well-defined period.

**QY Sge:** Menzies & Whitelock (1988) reported low amplitude variations with a characteristic time-scale of 50 days. Rao, Goswami & Lambert (2002) interpreted their spectra in terms of an obscured RV Tauri variable. The NSVS data are quite noisy but show four distinct minima of 0.08 mag at 60 days from each other.

**HD 213985:** Whitelock et al. (1989) observed a remarkably regular variability in  $K$ -band with a period of 254 d and a peak-to-peak amplitude  $\Delta K = 0.29$  mag. Van Winckel, Waelkens & Waters (2000) measured an orbital period of 259 d from long-term radial velocity measurements, implying that the light variations reflect orbital brightness modulation, either from variable extinction or light scattering. The ASAS data confirm the period and show a  $V$ -band amplitude ranging unpredictably between 0.2–0.6 mag (Fig. 4), which means the circumstellar shell must have variations on a similar time-scale to the orbital period. The power spectrum does not contain any excess power that could indicate low-amplitude pulsations.